High-Performance Paper-based Biocathode fabricated by Screen-printing an improved Mesoporous Carbon Ink and by Oriented Immobilization of Bilirubin Oxidase

Noya Loew
Isao Shitanda (shitanda@rs.tus.ac.jp)
Tokyo University of Science: Tokyo Rika Daigaku https://orcid.org/0000-0001-9751-016X
Himeka Goto
Hikari Watanabe
Tsutomu Mikawa
Seiya Tsujimura
Masayuki Itagaki

Research Article

Keywords: Paper-based biofuel cell, Screen-printing, Bilirubin oxidase, Bilirubin, Mesopo-rous carbon, Carboxymethyl cellulose

Posted Date: May 10th, 2022

DOI: https://doi.org/10.21203/rs.3.rs-1616157/v1

Abstract

In this study, the performance of a paper-based, screen-printed biofuel cell with mesoporous MgO-templated carbon (MgOC) electrodes was improved in two steps. First, a small amount of carboxymethyl cellulose (CMC) was added to the MgOC ink. Next, the cathode was modified with bilirubin prior to immobilizing the bilirubin oxidase (BOD). The CMC increased the accessibility of the mesopores of the MgOC, and subsequently, the performance of both the bioanode and biocathode. CMC also likely increased the stability of the electrodes. The pre-modification with bilirubin improved the orientation of the BOD, which facilitated direct electron transfer. With these two steps, an open circuit potential of 0.65 V, a maximal current density of 1.94 mA cm^{-2}, and a maximal power density of 465 µW cm^{-2} was achieved with lactate oxidase as bioanode enzyme and lactate as fuel. This is one of the highest reported performances for a biofuel cell.

1 Introduction

Mesoporous carbon materials are one of the most appealing materials for the fabrication of bioelectrochemical devices such as biosensors and biofuel cells [1–3]. These materials combine high conductivity, high surface area, and excellent biocompatibility, they are excellent for electrodes and matrices for enzyme immobilization. Yang et al. reported an increased temperature and pH stability when glucose oxidase was immobilized on ordered mesoporous carbon [4]. Among the different types of mesoporous carbon materials is MgO-templated carbon (MgOC), and it works excellently as its pore size can be controlled by controlling the size of the MgO template [5, 6]. The effect of the pore size of MgOC on the direct electrochemistry has been investigated for D-fructose dehydrogenase [7] and bilirubin oxidase (BOD) [8, 9]. Furthermore, biofuel cells (BFCs) fabricated with MgOC ink-modified carbon cloth had a high-power output of 2 mW cm^{-2} [10] and 4.3 mW cm^{-2} [11] with glucose dehydrogenase (GDH) and lactate oxidase (LOx) as enzymes, respectively.

A MgOC ink is also the first step in fabricating a screen-printed MgOC electrode. The conductive carbon material in screen-printing inks needs to be dispersed evenly under shear stress applied during printing. An uneven dispersion might lead to a partially brittle electrode (where too little binder is present) and/or a partially increased resistance (where too much binder is present). A higher dispersion can also lead to a higher degree of porosity, as clumping becomes less likely. Small quantities of additives can improve the dispersion of ink without interfering with the conductivity, and thus the quality and reproducibility of the printed electrode. However, although biocompatible and sustainable materials, such as carboxymethyl cellulose (CMC), have been used as dispersants for carbon materials [12], dispersants have not been considered for MgOC inks for screen-printing.

Screen-printed electrodes are promising for the fabrication of wearable biosensors, especially for healthcare applications [13–15]. Wearable biosensors are receiving significant attention in recent years owing to the trend of a more personalized, real-time healthcare management of patients, as well as a more data-driven, closer monitoring of the physical condition of high-performance professionals, such as

athletes and firefighters. Similarly, wearable BFCs are also receiving considerable attention, both as energy harvesters and self-powered sensors [16–19]. As energy harvesters, wearable BFCs collect energy from glucose or lactate contained in bodily fluids to power small devices. Wearable BFCs as self-powered sensors utilize the fact that the power collected from glucose or lactate at any time depends on the concentration of the respective fuel. Self-powered sensors do not require an energy source for the sensing device. Some examples of wearable biosensors and BFCs are integrated into the nose-pad of eyeglasses [20], microfluidics fabricated from a soft material [21, 22], fabricated on thin flexible film [22, 23], tattoo-type [24], textile-based [25, 26], and paper-based [27–29].

Paper-based devices also integrate the wicking effect of paper and can work with small sample volumes. del Torno-de Román et al. utilized paper as a fuel delivery system and achieved a power density of up to 37.5 μW cm^{-2} with 5 mM glucose [30]. Lau et al. used filter paper for fuel delivery and carbon fiber or carbon nanotube paper for the bioelectrodes and achieved a power density of 35.5 μW cm^{-2} with cascade-type 4-electron oxidation of ethanol and 26.9 μW cm^{-2} with formate, formaldehyde, and methanol as fuel and three cascade enzymes [31]. Rewatkar et al. also used filter paper for fuel delivery and multiwall carbon nanotube paper for the bioelectrodes and achieved a power density of 46.4 μW cm^{-2} with 30 mM glucose as fuel in a 4-cell-series configuration [32].

Our group has developed several BFCs with electrodes directly printed on Japanese paper. Using Ketjenblack as electrode material and glucose oxidase as anode-enzyme, we achieved a power density of 0.12 mW cm^{-2} [33]. Using MgOC as electrode material and lactate oxidase (Lox) as an enzyme, we achieved a power density of 0.113 mW cm^{-2} [28]. Using GDH as an enzyme and improving immobilization, we achieved a power density of 0.12 mW cm^{-2} [29]. These studies focused mainly on the anode performance. However, with a high-performing anode, the focus needs to shift to improving the cathode, especially in the case of self-powered biosensors, which need to be anode-limited in their performance.

A popular enzyme for constructing biocathode is bilirubin oxidase (BOD). One advantage of this enzyme is its capability for direct electron transfer (DET) [34–36]. As with all DET-type enzyme electrodes, the orientation of the enzyme on the electrode surface is crucial. Compared to a flat surface, a mesoporous surface structure increases the chances of the active site of a randomly oriented enzyme being within DET distance [37]; a directed orientation would increase the performance of a DET-type biocathode. Lalaoui et al. achieved an ordered immobilization of BOD on carbon nanotubes by utilizing protoporphyrin IX as a “guide” for binding the enzyme [38]. Al-Lolage et al. engineered BOD to have cysteine at a specific site and used that cysteine for a directed, covalent immobilization [39].

In this study, we used two approaches for improving the performance of screen-printed, paper-based biofuel cells, especially the biocathode. We considered the addition of carboxymethyl cellulose (CMC) as a dispersant to the MgOC ink and investigated its rheological effect. Focusing on the biocathode, we considered bilirubin as a “guide” for immobilizing BOD in an oriented manner.

2 Materials And Methods

2.1 Materials

The following materials were used in the experiment: MgOC with different average pore sizes (CNovelTM, Toyo Tanso, Japan), polyvinylidene difluoride hexafluoropropylene copolymer (PVdF; KF polymer L#9305, 5% in NMP, Kureha Corporation Japan), 1-methylpyrrolidin-2-one (NMP, Wako Pure Chemical Industries, Japan), CMC (SLD-F1, Nippon Paper Industries, Japan), Japanese paper (Izumo Tokusengasenshi, Japan), water-repellent agent (Hajikkusu, Komensu, Japan), carbon ink (JELCOM CH-10, Jujo Chemicals, Japan), 1,2-Naphthoquinone (1,2-NQ, Kanto Chemical, Japan), BOD from Myrothecium verrucaria (BO "Amano" 3, Amano Enzyme Inc., Japan), and Lox, which was derived from Enterococcus faecium and recombinantly prepared as reported previously [11].

All other chemicals were of analytical grade.

2.2 MgO-templated porous carbon ink

MgOC ink was prepared by dispersing MgOC and PVdF (binder; 5–6 mL / 1 g MgOC) in NMP (solvent; 2.5 mL / 1 g MgOC) until a smooth paste was obtained. For ink containing CMC, PVdF, NMP, and CMC (0.027 g / 1 g MgOC) were pre-mixed thoroughly prior to adding the MgOC.

2.3 Screen-printing of paper-based biofuel cell electrodes

Electrodes for the paper-based biofuel cell were fabricated similar to a previously reported method [28]. Japanese paper was treated with a water-repellent agent and allowed to dry at room temperature for 12 h. Next, current collectors were screen-printed in 5 layers using carbon ink with an LS-150TV screen-printer (Newlong Seimitsu Kogyo Co. Ltd., Tokyo, Japan) and dried at 120 ºC for 12 h. The current collectors for biocathodes had 100 holes with a 0.5 mm diameter to facilitate oxygen supply [28]. Finally, 2 layers were printed using MgOC ink to form the electrodes, which were allowed to dry at room temperature for 2 d. The electrode size was 2.0 x 0.5 cm for both the bioanode and biocathode.

2.4 BFC Preparation

Electrodes were modified to form bioanodes and biocathodes similar to a previously reported method [28]. After treating with UV ozone for 15 min, the bioanode was modified by applying 20 µL 100 mM 1,2-NQ in acetonitrile and dried for 1 h. 20 µL containing 40 U LOx in 10 mM phosphate buffer was applied and the electrode was dried under reduced pressure for 1.5 h. After UV ozone treatment for 15 min, the biocathode was modified by applying 20 µL containing 5 U BOD in 10 mM phosphate buffer and dried for 1.5 h under reduced pressure. If indicated, prior to modification with BOD, 20 µL of a 0–20 mM bilirubin solution in 20 mM NaOH was applied to the electrode and dried for 1.5 h under reduced pressure.

2.5 Rheological Measurements

Strain dispersion of the MgOC inks was evaluated using a rheometer (MCR 102, Anton Paar, Japan) at an angular frequency of 1.0 rad s^{-1}, a shear strain range of 10^{-5}–10%, and a temperature of 25 ºC.

2.6 Electrochemical evaluation

The bioanode and biocathode were evaluated individually in three-electrode systems with a platinum wire as a counter electrode and an Ag/AgCl/saturated KCl electrode as reference. Cyclic voltammetry was performed with 1 M phosphate buffer as an electrolyte that contains 100 mM lactate for the bioanode. The scan rate was 10 mV s^{-1} and the potential range − 0.5–0.7 V for the bioanode and 0.7–-0.2 V for the biocathode. Chronoamperometry was performed at an operating potential of 0.3 V with a measuring time of 2,000 s. Biofuel cells were evaluated by linear sweep voltammetry in a controlled environment with a temperature of 36 ºC and a humidity of 70%.

3 Results And Discussion

3.1 CMC as dispersant in MgOC inks

To investigate CMC as an additive for MgOC inks, the viscoelastic properties of inks with and without CMC were characterized by applying shear stress (Fig. 1). When CMC was added to the ink, the crossover point of the storage and loss moduli shifted to a higher shear strain value (7.9×10^{-3}% without CMC and 2.1×10^{-2}% with CMC; Fig. 1). This indicates that CMC improved the dispersion and ink containing CMC was more stable at higher shear stress. These characteristics are beneficial for screen-printing.

Next, the MgOC inks with and without CMC were printed into electrodes, which were fabricated, modified, and characterized electrochemically (Figs. 2–4). Cyclic voltammograms of the individual biocathodes and bioanodes showed a slightly narrower peak separation when electrodes printed with MgOC ink containing CMC were used (Fig. 2). Chronoamperometric measurements showed a clear increased reduction and oxidation current for the biocathode and bioanode, respectively (Fig. 3). As a result, combined into a biofuel cell, the maximal current density doubled from 0.35 mA/cm^2 when electrodes were fabricated without CMC to 0.79 mA cm^{-2} when fabricated with CMC (Fig. 4). The maximal power density increased more than 2.5-fold from 92 µW cm^{-2} to 249 µW cm^{-2} by adding CMC to the MgOC ink.

Although the rheological measurements indicated that adding CMC to the MgOC ink might be beneficial for screen-printing, the difference does not explain this drastic increase in performance. Furthermore, CMC is highly hygroscopic and can improve enzyme stability [40]. The hygroscopicity can facilitate the supply of fuel to the enzyme and the stabilizing effect might prevent the loss of enzyme activity during the immobilization process. Both these properties have the potential to increase the performance of the resulting enzyme electrodes and can explain the drastic increase in the performance of the biofuel cell.

3.2 Directed BOD immobilization using bilirubin

To further improve the performance of the biocathode, BOD was immobilized on the MgOC in an orientation favorable for DET. During DET, the electrode takes over the role of bilirubin in providing electrons. Thus, an orientation wherein the bilirubin-binding site of BOD faces the electrode should be

favorable for DET. To achieve this orientation, bilirubin was first immobilized on MgOC, followed by BOD. With this method, bilirubin should act as a “guide” for the BOD immobilization and the bilirubin-binding site should face the MgOC surface.

Biocathodes were fabricated with different amounts of bilirubin as a guide for the BOD immobilization and characterized electrochemically (Fig. 5). Both the cyclic voltammetric and chronoamperometric results show that a small amount of bilirubin on the electrode leads to an increased reduction current, while a large amount leads to a reduced reduction current. A small amount of bilirubin acts successfully as a guide and helps the bilirubin-binding site of the BOD to face the MgOC surface. A large amount, however, seems to inhibit the ability of the electrode to provide electrons to the enzyme, possibly by acting as an insulating layer. The optimal amount of bilirubin as a guide for BOD immobilization was 20 nmol cm^{-2} (Fig. 5).

3.3 Characterization of lactate biofuel cell including improved biocathode

The optimized biocathode, which was fabricated using MgOC ink containing CMC and BOD and immobilized with bilirubin as a guide, was combined with a bioanode, which was fabricated using MgOC ink containing CMC with 1,2-NQ as mediator and LOx as an enzyme. The resulting biofuel cell showed an open circuit potential (OCP) of 0.65 V, a maximal current density (J_{max}) of 1.94 mA cm^{-2}, and a maximal power density (P_{max}) of 465 µW cm^{-2}. These values indicate that the BFC fabricated here is among the best performing BFCs using lactate as fuel (Table 1). When stored in ambient conditions at room temperature, the output power density decreased to approximately half of the as-prepared value in the first 24 h (Supplementary Material, Fig. S1). After the first day, however, the BFCs were extremely stable for at least another 3 days (Fig. S1). The drastic decrease in the first day is likely due to enzyme inactivation, as the storage conditions were ill-suited to keeping enzyme activity. The high stability from the second day onward suggests that a significant amount of the enzyme is stabilized greatly by immobilizing inside of the mesopores of the MgOC and/or by the CMC.

Table 1
Performance of lactate BFCs.

BFC Type	Anode[a,b]	Cathode[a]	OCP V	J_{max} mA cm^{-2}	P_{max} µW cm^{-2}	Ref.
tattoo-type	LOx/TTF	Pt	0.50	n.a.	44	[41]
carbon paper	LDH/MB	LOx/hemin	0.79	0.76	380	[42]
carbon paper/flow	LOx/$FcMe_2$-LPEI	Lc/An	0.73	1.920	364	[43]
textile-based	LOx/1,4-NQ	Ag	0.49	0.91	252	[26]
paper-based	LOx/1,2-NQ	BOD	0.597	n.a.	113	[28]
paper-based	LOx/1,2-NQ	BOD	0.65	1.94	465	this work

n.a.: not available; a enzymes: BOD: bilirubin oxidase; Lc: laccase; LDH: lactate dehydrogenase; LOx: lactate oxidase; b mediators: 1,2-NQ: 1,2-naphthoquinone; 1,4-NQ: 1,4-naphthoquinone; An: anthracene; FcMe2-LPEI: dimethylferrocene-modified linear polyethyleneimine; MB: methylene blue; TTF: tetrathiafulvalene.

4 Conclusion

In this study, the performance of a paper-based, screen-printed BFC was improved in two steps. First, the dispersibility of MgOC ink was improved by adding a small amount of CMC. The increased dispersibility was confirmed rheometrically. Thus, the fabricated BFCs showed an increased performance owing to better accessibility of the mesopores of the MgOC, as well as the stabilizing effect of CMC on enzymes. This stabilizing effect was also seen in the storage stability of the BFCs. Second, BOD was immobilized in an oriented manner using bilirubin as a guide. The resulting BFC showed an OCP of 0.65 V, a J_{max} of 1.94 mA cm^{-2}, and a P_{max} of 465 µW cm^{-2}, which is among the highest performance values reported to date for BFCs utilizing lactate as fuel. Although this study utilized lactate as fuel, LOx as anode enzyme, and 1,2-NQ as anode mediator, all improvements achieved should apply to other anode enzymes, mediators, and fuels.

Declarations

Acknowledgements

This work was partially supported by JST-ASTEP Grant Number JPMJTR21UF (IS, ST), JSPS KAKENHI Grant Number 21H03344 (IS, ST). We would like to thank Editage (www.editage.com) for English language editing.

Conflict of interest

There are no conflicts of interest to declare.

References

1. X. Yang, P. Qiu, J. Yang, Y. Fan, L. Wang, W. Jiang, X. Cheng, Y. Deng, W. Luo, Small, Mesoporous materials–based electrochemical biosensors from enzymatic to nonenzymatic. 17 (2019). https://doi.org/10.1002/smll.201904022, 1904022
2. M. Etienne, L. Zhang, N. Vilà, A. Walcarius, Electroanalysis, Mesoporous materials-based electrochemical enzymatic biosensors. 27, 2028–2054 (2015). https://doi.org/10.1002/elan.201500172
3. A. Sanati, M. Jalali, K. Raeissi, F. Karimzadeh, M. Kharaziha, S.S. Mahshid, S. Mahshid, Mikrochim. Acta, A review on recent advancements in electrochemical biosensing using carbonaceous nanomaterials. 186, 773 (2019). https://doi.org/10.1007/s00604-019-3854-2
4. X. Yang, W. Yuan, D. Li, X. Zhang, R.S.C. Adv., Study on an improved bio-electrode made with glucose oxidase immobilized mesoporous carbon in biofuel cells. 6, 24451–24457 (2016). https://doi.org/10.1039/C5RA27111H
5. T. Morishita, T. Tsumura, M. Toyoda, J. Przepiórski, A.W. Morawski, H. Konno, M. Inagaki, Carbon, A review of the control of pore structure in MgO-templated nanoporous carbons. 48, 2690–2707 (2010). https://doi.org/10.1016/j.carbon.2010.03.064
6. M. Inagaki, M. Toyoda, Y. Soneda, S. Tsujimura, T. Morishita, Carbon, Templated mesoporous carbons: Synthesis and applications. 107, 448–473 (2016). https://doi.org/10.1016/j.carbon.2016.06.003
7. H. Funabashi, K. Murata, S. Tsujimura, Electrochemistry, Effect of pore size of MgO-templated carbon on the direct electrochemistry of D-fructose dehydrogenase. 83, 372–375 (2015). https://doi.org/10.5796/electrochemistry.83.372
8. H. Funabashi, S. Takeuchi, S. Tsujimura, Hierarchical meso/macro-porous carbon fabricated from dual MgO templates for direct electron transfer enzymatic electrodes. Sci. Rep. **7**, 45147 (2017). https://doi.org/10.1038/srep45147
9. S. Tsujimura, M. Oyama, H. Funabashi, S. Ishii, Electrochim. Acta, Effects of pore size and surface properties of MgO-templated carbon on the performance of bilirubin oxidase–modified oxygen reduction reaction cathode. 322 (2019). https://doi.org/10.1016/j.electacta.2019.134744, 134744
10. A. Niiyama, K. Murata, Y. Shigemori, A. Zebda, S. Tsujimura, J.Power Sources, High-performance enzymatic biofuel cell based on flexible carbon cloth modified with MgO-templated porous carbon. 427, 49–55 (2019). https://doi.org/10.1016/j.jpowsour.2019.04.064
11. I. Shitanda, K. Takamatsu, A. Niiyama, T. Mikawa, Y. Hoshi, M. Itagaki, S. Tsujimura, J. Power, Sources, High-power lactate/O2 enzymatic biofuel cell based on carbon cloth electrodes modified with MgO-templated carbon. 436 (2019). https://doi.org/10.1016/j.jpowsour.2019.226844, 226844

12. R. Koshani, M. Tavakolian, T.G.M. van de Ven, Cellulose-based dispersants and flocculants. J. Mater. Chem. B **8**, 10502–10526 (2020). https://doi.org/10.1039/D0TB02021D
13. S. Khan, S. Ali, A. Bermak, Sensors (Basel), Recent developments in printing flexible and wearable sensing electronics for healthcare applications. 19, 1230 (2019). https://doi.org/10.3390/s19051230
14. P. Yáñez-Sedeño, S. Campuzano, J.M. Pingarrón, Biosensors, Screen-printed electrodes: Promising paper and wearable transducers for (bio)sensing. 10, 76 (2020). https://doi.org/10.3390/bios10070076
15. M. Chung, G. Fortunato, N. Radacsi, J. R. Soc. Interface, Wearable flexible sweat sensors for healthcare monitoring: A review. 16, 20190217 (2019). https://doi.org/10.1098/rsif.2019.0217
16. E. Katz, A.F. Bückmann, I. Willner, J. Am. Chem. Soc., Self-powered enzyme-based biosensors. 123, 10752–10753 (2001). https://doi.org/10.1021/ja0167102
17. I. Shitanda, M. Momiyama, N. Watanabe, T. Tanaka, S. Tsujimura, Y. Hoshi, M. Itagaki, ChemElectroChem, Toward Wearable Energy Storage Devices: Paper-Based Biofuel Cells based on a Screen-Printing Array Structure. 4, 2460–2463 (2017). https://doi.org/10.1002/celc.201700561
18. I. Shitanda, S. Tsujimura, J. Phys. Energy, Toward self-powered real-time health monitoring of body fluid components based on improved enzymatic biofuel cells. 3 (2021). https://doi.org/10.1088/2515-7655/abebcb, 032002
19. M. Parrilla, K. De Wael, Wearable self-powered electrochemical devices for continuous health management. Adv. Funct. Mater. **31**, 2107042 (2021). https://doi.org/10.1002/adfm.202107042
20. J.R. Sempionatto, T. Nakagawa, A. Pavinatto, S.T. Mensah, S. Imani, P. Mercier, J. Wang, Lab Chip, Eyeglasses based wireless electrolyte and metabolite sensor platform. 17, 1834–1842 (2017). https://doi.org/10.1039/C7LC00192D
21. A. Koh, D. Kang, Y. Xue, S. Lee, R.M. Pielak, J. Kim, T. Hwang, S. Min, A. Banks, P. Bastien, M.C. Manco, L. Wang, K.R. Ammann, K.I. Jang, P. Won, S. Han, R. Ghaffari, U. Paik, M.J. Slepian, G. Balooch, Y. Huang, J.A. Rogers, Sci. Transl. Med., A soft, wearable microfluidic device for the capture, storage, and colorimetric sensing of sweat. 8, 366ra165–366ra165 (2016). https://doi.org/10.1126/scitranslmed.aaf2593
22. I. Shitanda, M. Mitsumoto, N. Loew, Y. Yoshihara, H. Watanabe, T. Mikawa, S. Tsujimura, M. Itagaki, M. Motosuke, Electrochim. Acta, Continuous sweat lactate monitoring system with integrated screen-printed MgO-templated carbon-lactate oxidase biosensor and microfluidic sweat collector. 368 (2021). https://doi.org/10.1016/j.electacta.2020.137620, 137620
23. T. Minamiki, S. Tokito, T. Minami, Fabrication of a flexible biosensor based on an organic field-effect transistor for lactate detection. Anal. Sci. **35**, 103–106 (2019). https://doi.org/10.2116/analsci.18SDN02
24. W. Jia, A.J. Bandodkar, G. Valdés-Ramírez, J.R. Windmiller, Z. Yang, J. Ramírez, G. Chan, J. Wang, Anal. Chem., Electrochemical tattoo biosensors for real-time noninvasive lactate monitoring in human perspiration. 85, 6553–6560 (2013). https://doi.org/10.1021/ac401573r

25. R. Wang, Q. Zhai, T. An, S. Gong, W. Cheng, Talanta, Stretchable gold fiber-based wearable textile electrochemical biosensor for lactate monitoring in sweat. 222, 121484 (2021). https://doi.org/10.1016/j.talanta.2020.121484
26. J. Lv, I. Jeerapan, F. Tehrani, L. Yin, C.A. Silva-Lopez, J.-H. Jang, D. Joshuia, R. Shah, Y. Liang, L. Xie, F. Soto, C. Chen, E. Karshalev, C. Kong, Z. Yang, J. Wang, Sweat-based wearable energy harvesting-storage hybrid textile devices. Energy Environ. Sci. **11**, 3431–3442 (2018). https://doi.org/10.1039/C8EE02792G
27. N. Colozza, K. Kehe, G. Dionisi, T. Popp, A. Tsoutsoulopoulos, D. Steinritz, D. Moscone, F. Arduini, Biosens. Bioelectron., A wearable origami-like paper-based electrochemical biosensor for sulfur mustard detection. 129, 15–23 (2019). https://doi.org/10.1016/j.bios.2019.01.002
28. I. Shitanda, Y. Morigayama, R. Iwashita, H. Goto, T. Aikawa, T. Mikawa, Y. Hoshi, M. Itagaki, H. Matsui, S. Tokito, S. Tsujimura, J.Power Sources, Paper-based lactate biofuel cell array with high power output. 489 (2021). https://doi.org/10.1016/j.jpowsour.2021.229533, 229533
29. I. Shitanda, Y. Fujimura, T. Takarada, R. Suzuki, T. Aikawa, M. Itagaki, S. Tsujimura, ACS Sens., Self-powered diaper sensor with wireless transmitter powered by paper-based biofuel cell with urine glucose as fuel. 6, 3409–3415 (2021). https://doi.org/10.1021/acssensors.1c01266
30. L. del Torno-de Román, M. Navarro, G. Hughes, J.P. Esquivel, R.D. Milton, S.D. Minteer, N. Sabaté, Electrochim. Acta, Improved performance of a paper-based glucose fuel cell by capillary induced flow. 282, 336–342 (2018). https://doi.org/10.1016/j.electacta.2018.05.074
31. C. Lau, M.J. Moehlenbrock, R.L. Arechederra, A. Falase, K. Garcia, R. Rincon, S.D. Minteer, S. Banta, G. Gupta, S. Babanova, P. Atanassov, Paper based biofuel cells: Incorporating enzymatic cascades for ethanol and methanol oxidation. Int. J. Hydrogr Energy **40**, 14661–14666 (2015). https://doi.org/10.1016/j.ijhydene.2015.06.108
32. P. Rewatkar, U.S.,J.S. Goel, A.C.S. Sustain, Chem. Eng., Optimized shelf-stacked paper origami-based glucose biofuel cell with immobilized enzymes and a mediator. 8, 12313–12320 (2020). https://doi.org/10.1021/acssuschemeng.0c04752
33. I. Shitanda, S. Kato, Y. Hoshi, M. Itagaki, S. Tsujimura, (Camb), Flexible and high-performance paper-based biofuel cells using printed porous carbon electrodes. Chem. Commun. **49**, 11110–11112 (2013). https://doi.org/10.1039/C3CC46644B
34. S. Shleev, A. Elkasmi, T. Ruzgas, L. Gorton, Electrochem. Commun., Direct heterogeneous electron transfer reactions of bilirubin oxidase at a spectrographic graphite electrode. 6, 934–939 (2004). https://doi.org/10.1016/j.elecom.2004.07.008
35. S. Brocato, C. Lau, P. Atanassov, Electrochim. Acta, Mechanistic study of direct electron transfer in bilirubin oxidase. 61, 44–49 (2012). https://doi.org/10.1016/j.electacta.2011.11.074
36. C.H. Kjaergaard, F. Durand, F. Tasca, M.F. Qayyum, B. Kauffmann, S. Gounel, E. Suraniti, K.O. Hodgson, B. Hedman, N. Mano, E.I. Solomon, Spectroscopic and crystallographic characterization of “alternative resting” and “resting oxidized” enzyme forms of bilirubin oxidase: Implications for

activity and electrochemical behavior of multicopper oxidases. J. Am. Chem. Soc. **134**, 5548–5551 (2012). https://doi.org/10.1021/ja211872j

37. Y. Sugimoto, Y. Kitazumi, O. Shirai, K. Kano, Electrochemistry, Effects of mesoporous structures on direct electron transfer-type bioelectrocatalysis: Facts and simulation on a three-dimensional model of random orientation of enzymes. 85, 82–87 (2017). https://doi.org/10.5796/electrochemistry.85.82
38. N. Lalaoui, A. Le Goff, M. Holzinger, S. Cosnier, Chemistry, Fully oriented bilirubin oxidase on porphyrin-functionalized carbon nanotube electrodes for electrocatalytic oxygen reduction. 21, 16868–16873 (2015). https://doi.org/10.1002/chem.201502377
39. F.A. Al-Lolage, P.N. Bartlett, S. Gounel, P. Staigre, N. Mano, ACS Catal., Site-directed immobilization of bilirubin oxidase for electrocatalytic oxygen reduction. 9, 2068–2078 (2019). https://doi.org/10.1021/acscatal.8b04340
40. J. Li, Z. Jiang, H. Wu, Y. Liang, Y. Zhang, J. Liu, Carbohydr. Polym., Enzyme–polysaccharide interaction and its influence on enzyme activity and stability. 82, 160–166 (2010). https://doi.org/10.1016/j.carbpol.2010.04.045
41. W. Jia, G. Valdés-Ramírez, A.J. Bandodkar, J.R. Windmiller, J. Wang, Angew. Chem. Int Ed Engl, Epidermal biofuel cells: Energy harvesting from human perspiration. 52, 7233–7236 (2013). https://doi.org/10.1002/anie.201302922
42. A. Koushanpour, M. Gamella, E. Katz, Electroanalysis, A biofuel cell based on biocatalytic reactions of lactate on both anode and cathode electrodes – Extracting electrical power from human sweat. 29, 1602–1611 (2017). https://doi.org/10.1002/elan.201700126
43. R.A. Escalona-Villalpando, R.C. Reid, R.D. Milton, L.G. Arriaga, S.D. Minteer, J. Ledesma-García, J. Power Sources, Improving the performance of lactate/oxygen biofuel cells using a microfluidic design. 342, 546–552 (2017). https://doi.org/10.1016/j.jpowsour.2016.12.082

Figures

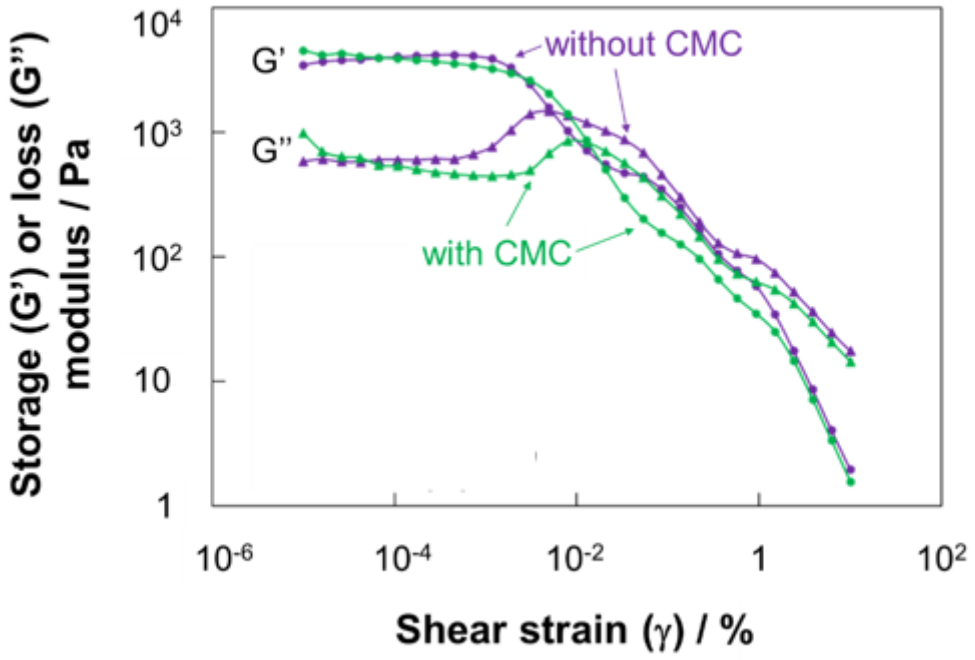

Figure 1

Storage and loss modulus of MgOC inks with or without CMC as a function of shear strain. Angular frequency: 1.0 rad s^{-1}; temperature 25 °C. Circles: storage modulus (G'); triangles: loss modulus (G"); green: MgOC ink containing CMC; violet: MgOC ink without CMC.

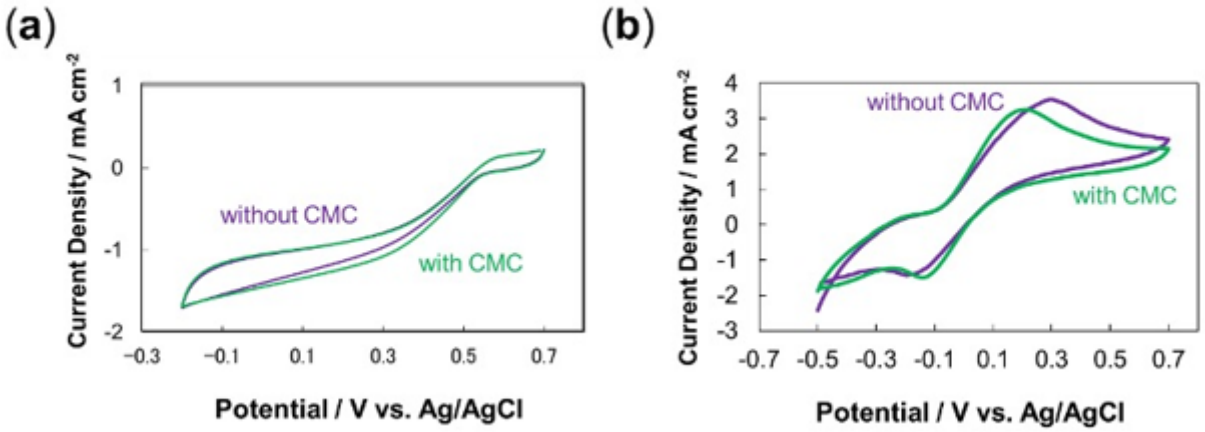

Figure 2

Cyclic voltammograms of (a) biocathodes, and (b) bioanodes, fabricated using MgOC inks with and without CMC. Scan rate: 10 mV s^{-1}; 1 M phosphate buffer, pH 7.0; (b) 100 mM lactate. Biocathode

enzyme: BOD; bioanode enzyme: LOx; bioanode mediator 1,2-NQ. Green: with CMC; violet: without CMC.

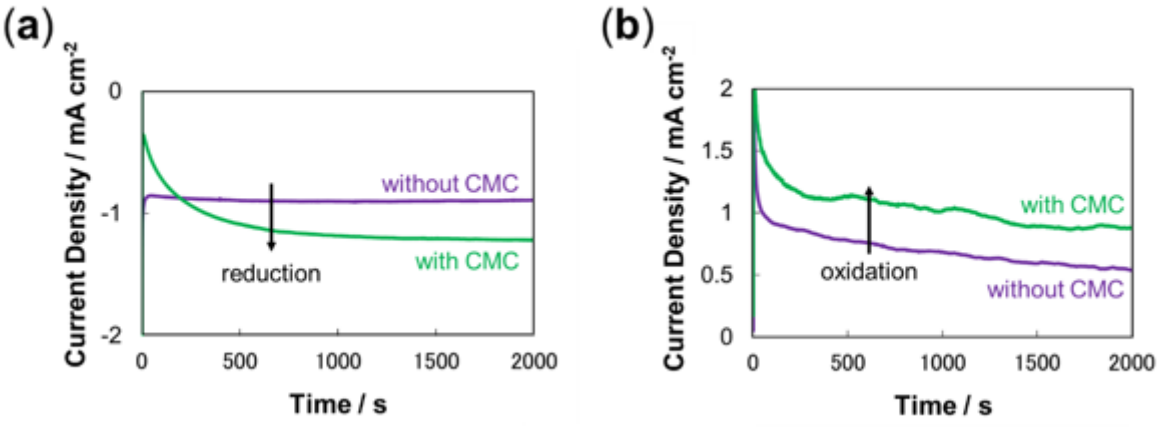

Figure 3

Electrochemical evaluation of (a) biocathodes, and (b) bioanodes fabricated using MgOC inks with and without CMC. 1 M phosphate buffer, pH 7.0; 0.3 V vs Ag/AgCl/sat. KCl; room temperature. (b) 100 mM lactate. (a) BOD; (b) LOx, 1,2-NQ. Green: with CMC; violet: without CMC.

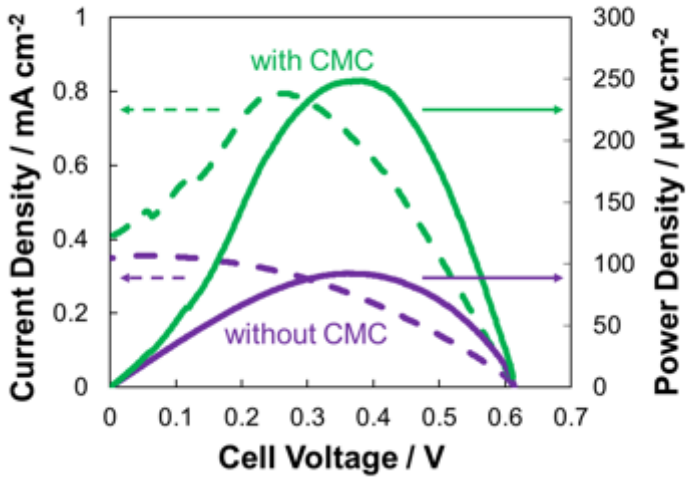

Figure 4

Electrochemical evaluation of biofuel cells fabricated using MgOC inks with and without CMC. 1 M phosphate buffer, pH 7.0; 100 mM lactate; humidity 70%; temperature 36 ºC. Biocathode enzyme: BOD;

bioanode enzyme: LOx; bioanode mediator 1,2-NQ. Green: with CMC; violet: without CMC; straight line: power density; dashed line: current density.

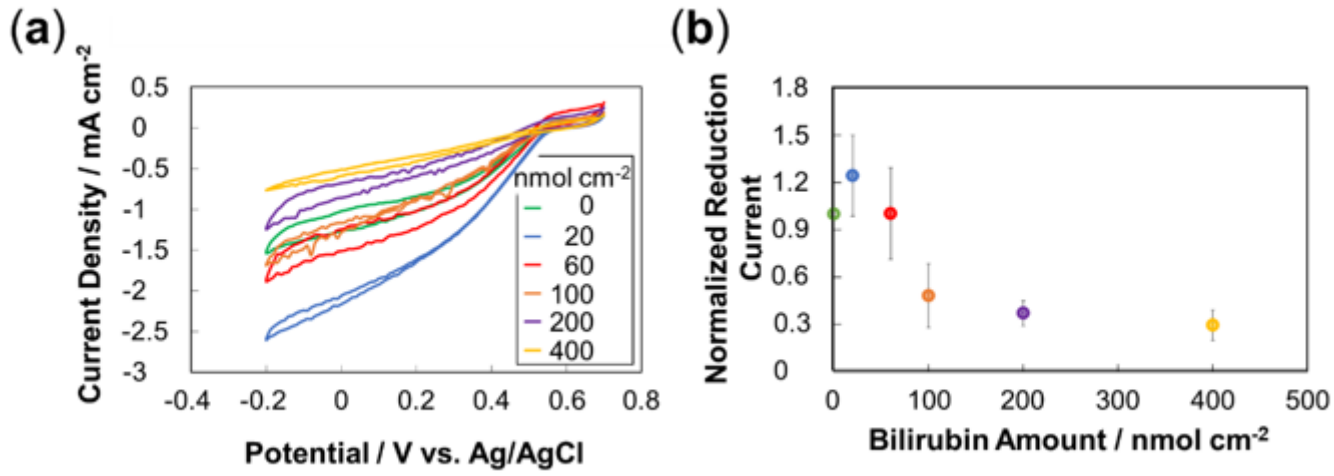

Figure 5

Electrochemical evaluation of biocathodes with BOD adsorbed on MgOC with bilirubin as guide for orientation. CE = Pt wire; RE = Ag/AgCl/sat. KCl; 1 M phosphate buffer, pH 7.0. (a) Cyclic voltammograms. Legend: bilirubin amount. (b) Normalized reduction current obtained chronoamperometrically vs. bilirubin amount used for immobilizing BOD. 0.3 V vs. Ag/AgCl/sat. KCl. Current for electrode with BOD immobilized in absence of bilirubin = 1.

Supplementary Files

This is a list of supplementary files associated with this preprint. Click to download.

- BFCcathodeSuplMater.docx